Spin and charge dynamics in $[TbPc_2]^0$ and $[DyPc_2]^0$ single molecule magnets

F. Branzoli[1], P. Carretta[1], M. Filibian[1], M. J. Graf[2], S. Klyatskaya[3], M. Ruben[3,4], F. Coneri[5] and P. Dhakal[2].

[1]*Department of Physics "A. Volta", University of Pavia-CNISM, 27100 Pavia (Italy)*
[2]*Department of Physics, Boston College, 02467 USA*
[3]*Institute of Nanotechnology, Karlsruhe Institute of Technology (KIT), 76344 Eggenstein-Leopoldshafen (Germany)*
[4]*IPCMS-CNRS UMR 7504, Université de Strasbourg, 67034 Strasbourg (France) and*
[5]*Department of Physics, University of Parma-CNISM, 43100 Parma (Italy)*

Magnetization, AC susceptibility and μSR measurements have been performed in neutral phthalocyaninato lanthanide ($[LnPc_2]^0$) single molecule magnets in order to determine the low-energy levels structure and to compare the low-frequency spin excitations probed by means of macroscopic techniques, such as AC susceptibility, with the ones explored by means of techniques of microscopic character, such as μSR. Both techniques show a high temperature thermally activated regime for the spin dynamics and a low temperature tunneling one. While in the activated regime the correlation times for the spin fluctuations estimated by AC susceptibility and μSR basically agree, clear discrepancies are found in the tunneling regime. In particular, μSR probes a faster dynamics with respect to AC susceptibility. It is argued that the tunneling dynamics probed by μSR involves fluctuations which do not yield a net change in the macroscopic magnetization probed by AC susceptibiliy. Finally resistivity measurements in $[TbPc_2]^0$ crystals show a high temperature nearly metallic behaviour and a low temperature activated behaviour.

I. INTRODUCTION

The trend towards ever-smaller electronic devices is driving electronics to its ultimate molecular-scale limit, which allows for the exploitation of quantum effects. Single Molecule Magnets (SMM) are among the most promising materials to be used in molecular spintronic devices[1] or as logic units in quantum computers[2], since they combine the classical macroscale properties of bulk magnetic materials with the advantages of nanoscale entities, such as quantum coherence. It has already been shown theoretically[2] that molecular magnets can be used to build efficient memory devices[3] and, in particular, one single molecule can serve as a storage unit of a dynamic random access memory device[4,5]. In addition, SMM have been recognized as suitable materials which can be used as contrast agents for medical diagnostics. In fact, these molecules comprise the chemical and magnetic structure of the gadolinium chelates with the superparamagnetism of the SPIOs (Superparamagnetic Iron Oxides), materials which represent some of the most common MRI contrast agents in current use[6].

$LnPc_2$-based compounds ($Pc=C_{32}H_{16}N_8$ is phthalocyanine, Ln a lanthanide ion) represent a new class of SMM characterized by a doubly-degenerate ground state and large magnetic anisotropy which yields a remarkably large barrier to spin reversal. In particular, $[TbPc_2]^-$ and $[DyPc_2]^-$ complexes are the first mononuclear systems exhibiting a very slow relaxation of magnetization[7] and consequently a characteristic correlation time (τ_c) for the spin fluctuations reaching several μs at liquid nitrogen temperature. At variance with transition metal molecular magnets, in the $LnPc_2$ molecules the electronic levels of the ground-state multiplet, with angular momentum J, are mainly split by the strong anisotropy of

the crystal field (CF) at the Ln^{3+} ion. Accordingly the separation between the double degenerate ground state and the first excited levels can reach several hundreds of kelvin, thus yielding unprecedently large τ_c at cryogenic temperatures. Moreover, it is noticed that the magnetic properties of these lanthanide complexes are strongly influenced by the chemical and structural modification of the ligands through which the CF potential can be varied[8]. The CF configuration can be modified from the very dilute limit in $[LnPc_2]^-[TBA]^+N[TBA]Br$, with N+1 $\gg$ 1 the number tetrabutylammonia units, to the concentrated limit consisting solely of neutral double-decker molecules $[LnPc_2]^0$. Recently it has been shown that one or two-electron oxidation of $[LnPc_2]^-$ yields a compression of the cage around Ln^{3+} ion and an increase of the CF splitting[9,10,11].

By means of nuclear magnetic resonance (NMR) and muon spin relaxation (μSR), the correlation time for the spin fluctuations in the neutral compounds $[TbPc_2]^0$ and $[DyPc_2]^0$ was found to be close to 0.1 ms at 50 K[12], about two orders of magnitude larger than the one previously observed in the non-oxidized lanthanide based single molecule magnets. In $[TbPc_2]^0$ two different regimes for the spin fluctuations have been evidenced: a high temperature thermally activated regime involving spin fluctuations, driven by spin-phonon coupling, across a barrier $\Delta \simeq 880$ K separating the $|J = 6, m = \pm6\rangle$ ground states and the $|J = 6, m = \pm5\rangle$ first excited states, and a low temperature regime involving quantum fluctuations within the twofold degenerate ground-state. For $[DyPc_2]^0$ a high temperature thermally activated regime is also found, however it cannot be explained in terms of a single spin-phonon coupling constant.

Here we report an analysis of the static uniform spin susceptibility (χ_S) for the $[DyPc_2]^0$ complex, from which

a determination of the low energy level structure of the Dy^{3+} ion spin multiplet J=15/2 is made. On the basis of these results for the CF level splitting it is possible to analyze the temperature (T) dependence of muon spin-lattice relaxation rate in the presence of an applied field, derived from previous μSR measurements performed at the ISIS facility[12] and from new measurements performed at the Paul Scherrer Institute (PSI). Accordingly, the spin-phonon couplings driving the transitions among the CF levels have been derived and the characteristic correlation time for the spin fluctuations estimated. μSR results are compared to the ones obtained by AC susceptibility measurements in the same samples. It is found that both AC susceptibility and μSR probe a high temperature activated and a low temperature tunneling regime for the spin dynamics. However, while the values estimated for the correlation times in the high temperature activated regime are quite close, at low temperature the tunneling rate probed by μSR is much faster than the one derived by AC susceptibility. Finally, transport measurements in $[TbPc_2]^0$ crystals are presented.
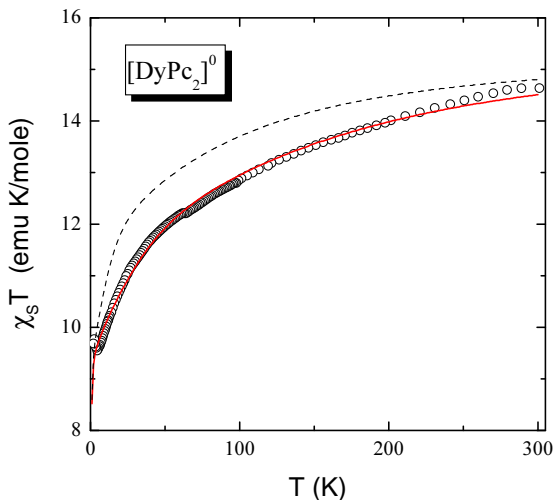

FIG. 1: Temperature dependence of χT in $[DyPc_2]^0$ for H = 1000 Gauss (open circles) and the best fit curve calculated according to Eq.1 curve (solid line). The dashed line corresponds to the behaviour calculated on the basis of $[DyPc_2]^- TBA^+$ CF splittings derived by Ishikawa et al. [13]

II. TECHNICAL ASPECTS AND EXPERIMENTAL RESULTS

All reagents were purchased from Across or Aldrich and used without further purification. The synthesis of both samples was carried out by using several modifications of the protocol based on the published procedure reported in Ref.14. The synthesis was accomplished by templating reactions, starting from a mixture of the phthalonitrile precursor o-dicyanobenzene and the lanthanide acetylacetonate $Ln(acac)_3 \cdot nH_2O$,

in the presence of a strong base (e.g. DBU, alkoxides) and high-boiling solvents, such as pentanol or hexanol. A mixture of 1,2-dicyanobenzene (42 mmol), $Ln(acac)_3 \cdot 4H_2O$ (Ln = Tb^{3+}, Dy^{3+}) (5 mmol), and 1,8-diazabicyclo[5,4,0]undec-7-ene (DBU) (21 mmol) in 50 mL of 1-pentanol was refluxed for 1.5 days. The solution was allowed to cool to room temperature and then acetic acid was added and the mixture was heated at 100 C for 0.5 hours. The precipitate was collected by filtration and washed with n-hexane and Et_2O. The crude purple product was redissolved in 800 Ml of $CHCl_3/MeOH$ (1/1) and the undissolved PcH_2 was filtered off. Both forms, blue (anionic $[LnPc_2]^-$) and green (neutral $[LnPc_2]^0$), were obtained simultaneously, as revealed by electronic absorption spectra[14]. In order to convert the unstabilized anionic form to the neutral one, the reaction mixture was presorbed on active (H_2O-0%) basic alumina oxide. Purification was carried out by column chromatography on basic alumina oxide (deactivated with 4.6 % H_2O, level IV) with chlorophorm-methanol mixture (10:1) as eluent. In general, the yield was 30-35%. By means of additional radial chromatography on silica gel followed by recrystallization from chloroform-hexane mixture, analytically pure powder samples were achieved.

Deep green crystals of the products were obtained by using slow diffusion of CH_2Cl_2 into $C_2H_2Cl_4$ solution of the pristine $[LnPc_2]^0$. After 2 weeks, deep green needle-like crystals were obtained (see Fig.2). The $[LnPc_2]^0$ molecules crystallized in the space group $P2_12_12_1$ (γ-phase) as reported in Ref.15 and were isomorphous to each other.
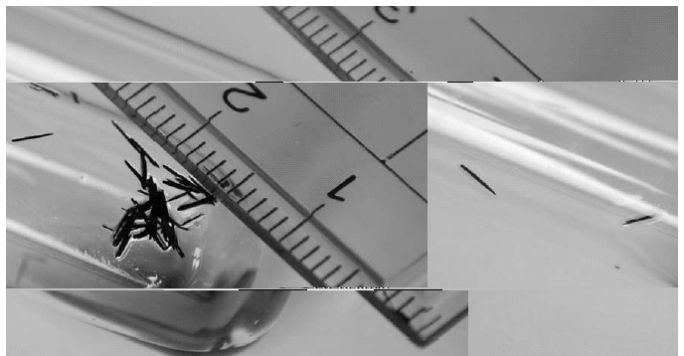

FIG. 2: Photograph of a few $[TbPc_2]^0$ crystals grown according to the procedure reported above. The numbers in the ruler scale correspond to centimeters.

DC Magnetization (M) and AC susceptibility measurements have been performed by means of an MPMS-XL7 Quantum Design SQUID magnetometer. The static uniform susceptibility was determined from the ratio $\chi_S = M/H$ in an applied field H = 1000 G in the 2-300 K temperature range. In Fig. (1) the T dependence of χ_ST is shown. In-phase (χ'-real) and out-of-phase (χ''-imaginary) AC susceptibility data were collected at oscillating field frequencies between 10 and 1488 Hz, in the 10-

80 K temperature range and for different applied static fields. In Fig. (3) the temperature and frequency dependence of the AC susceptibility for $[TbPc_2]^0$ is shown. A sharp drop in $\chi' T$ is observed on cooling in correspondence to a peak in χ''/χ_S, which progressively shifts to lower temperatures as the AC frequency is lowered. In $[DyPc_2]^0$ analogous but slightly broader peaks are observed at lower temperature (Fig. 4), suggesting a faster dynamic (see Discussion).

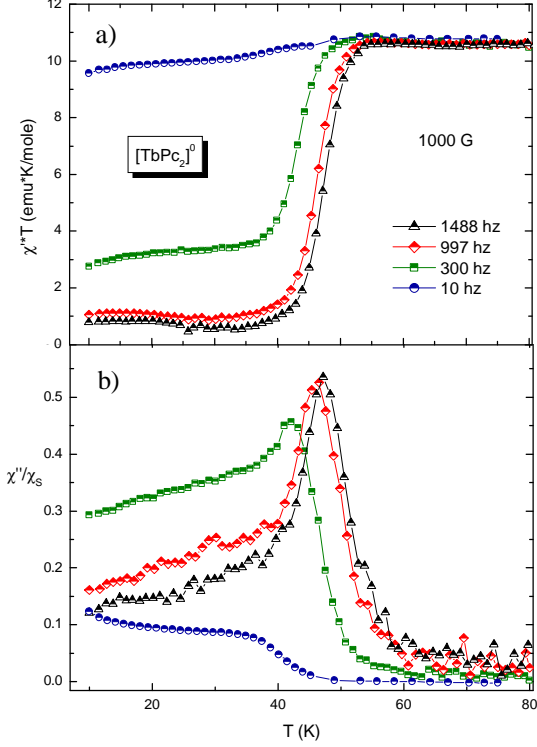FIG. 3: Temperature dependence of a) $\chi' T$ and b) χ''/χ_S in $[TbPc_2]^0$, where χ', χ'' and χ_S are in-phase-AC, out-of-phase-AC and DC molar magnetic susceptibilities, respectively. The measurements were performed in 4 G oscillating magnetic field at 10, 300, 997 and 1488 Hz, in the presence of a 1000 G DC component.

Longitudinal field μSR measurements in the 50 mK-300 K temperature range were carried out either at ISIS pulsed muon facility on MuSR beam line[12], or at PSI muon facility on GPS (General Purpose Surface-Muon Instrument) and LTF (Low Temperature Facility) beam lines. In contrast to the ISIS measurements, the continuous beam muon production at PSI allows for a much more accurate determination of the short-time relaxation. In Fig. (5) zero-field (ZF) depolarization curves at a few selected temperatures are shown for $[DyPc_2]^0$. A Kubo-Toyabe (KT) relaxation[16] is clearly observed below $T^* \simeq 60$ K, indicating very slow fluctuations, that is, $\nu/(\gamma_\mu \sqrt{\langle \Delta h_\perp^2 \rangle_\mu}) \ll 1$, with $\nu = 1/\tau_c$ being the characteristic frequency of the spin fluctuations and $\langle \Delta h_\perp^2 \rangle_\mu$ is the mean squared amplitude of the field fluctuations at the muon site. γ_μ is the muon gyromagnetic ratio. By fitting
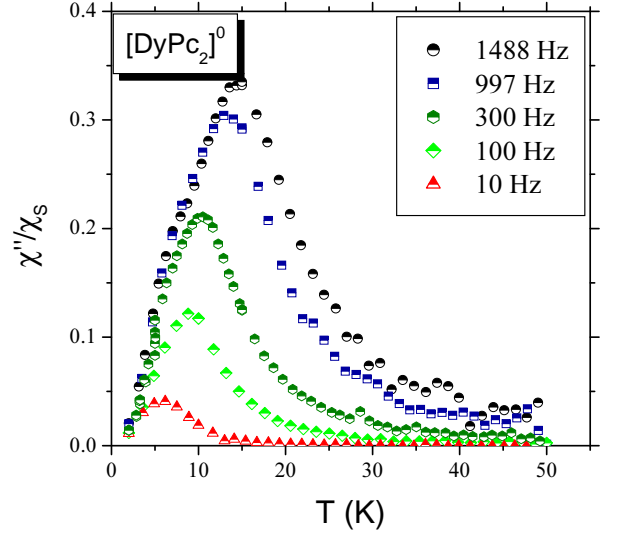

FIG. 4: Temperature dependence of the normalized out-of-phase spin susceptibility χ''/χ_S in $[DyPc_2]^0$, for a 4 G oscillating magnetic field at various frequencies. A 9000 G static external field was applied.
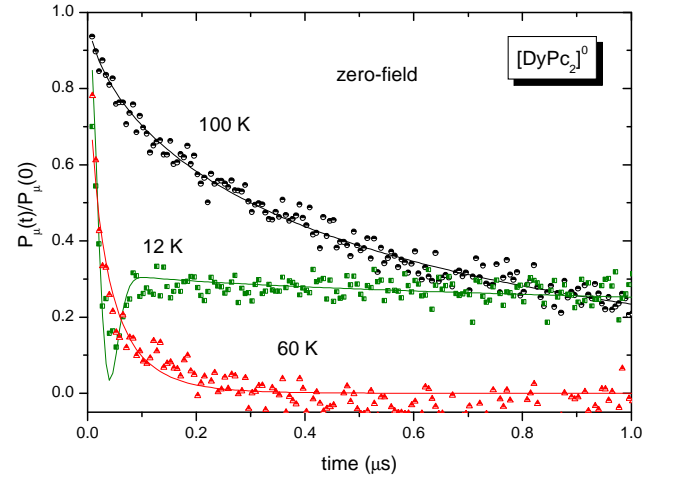

FIG. 5: Time evolution of the muon polarization in zero-field in $[DyPc_2]^0$ sample normalized to its value for t $\rightarrow$ 0 at three selected temperatures.

the low-temperature data with a KT function one can estimate the static field distribution probed by the muons around $\sqrt{\langle \Delta h_\perp^2 \rangle_\mu} = 490$ G and $\sqrt{\langle \Delta h_\perp^2 \rangle_\mu} = 550$ G for the Dy and Tb compounds, respectively. These values are in excellent agreement with the measured "repolarization" of the signals with applied longitudinal fields. In the slow fluctuations regime only the 1/3 tail of the KT depolarization function is affected by slow fluctuations and it decays according to $P_\mu(t) = exp(-(2/3)\nu t) = exp(-\lambda t)$. On the other hand, for $T > T^*$ (around 60 K for $[DyPc_2]^0$ and around 90 K for $[TbPc_2]^0$) the fast fluctuations limit is attained. In this limit the decay of the polarization in zero or in a longitudinal field is given by $P_\mu(t) = exp(-2\gamma_\mu^2 \langle \Delta h_\perp^2 \rangle_\mu t/\nu)^\beta = exp(-\lambda t)^\beta$, where

the exponent β can differ from unity in case of a distribution of muon sites, as it can be the case here. In the intermediate fluctuation limit $\nu/(\gamma_\mu\sqrt{\langle\Delta h_\perp^2\rangle_\mu}) \geq 1$ (T$\simeq$T*), λ starts to decrease according to the so-called Abragam form[16].
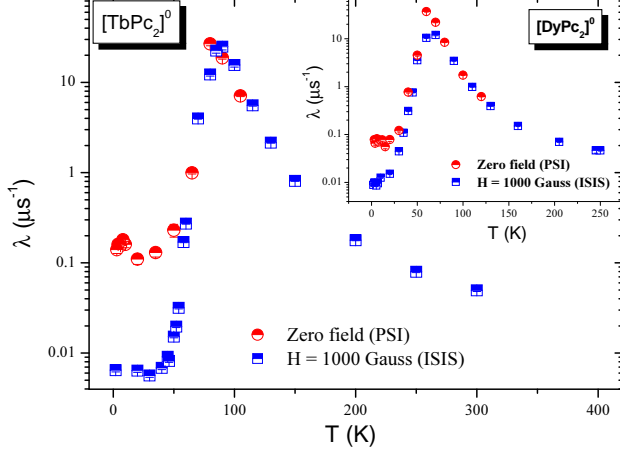

FIG. 6: T dependence of the muon ZF longitudinal relaxation rate (circles) in $[TbPc_2]^0$ and $[DyPc_2]^0$ (in the inset), together with 1000 G longitudinal field data from Ref. 12 (squares).

By using the aforementioned expressions for the decay of the polarization in the fast and slow fluctuations regime it was possible to derive the T-dependence of λ (Fig.6) in zero-field and estimate the T-dependence of τ_c (see Fig. 7), which was compared with the one previously derived at ISIS for a 1000 G longitudinal field[12]. The data for both materials were fit with a stretched exponential above T*, with a T-independent exponent $\beta = 0.5$. In Fig. 7 one notices that in the high T regime the τ_c derived in zero-field and in a 1000 Gauss longitudinal field are in satisfactory agreement and show an activated T-dependence of τ_c. On the other hand, below 50 K, where tunneling processes become relevant, $\tau_c(T)$ is observed to flatten at values which differ by more than an order of magnitude upon increasing the field from zero to 1000 G. The increase of τ_c with the magnetic field intensity, also observed in the AC-susceptibility measurements (Discussion), should be ascribed to the removal of the ground-state degeneracy by the magnetic field, which progressively inhibits the tunneling processes.

Data taken below 1 K in LTF yield an essentially temperature independent depolarization rate for both complexes down to 50 mK, as expected for tunneling dominated depolarization. However, there exists a weak maximum in $\lambda(T)$, near T = 0.2 K for the Dy sample and near T = 0.7 K for the Tb sample, which warrant further studies (Fig. (8) and see Discussion).

Resistivity measurements on single crystal samples of $[TbPc_2]^0$, with current along the c-axis, have been performed in the 2.8 - 294 K temperature range in DC mode by using a four-terminal technique. Contacts were made
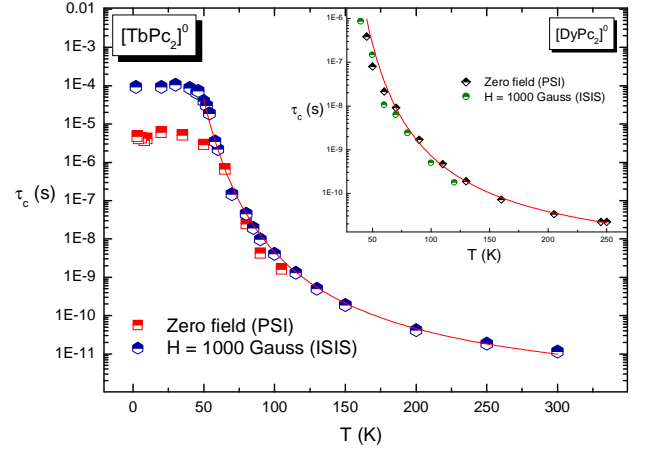

FIG. 7: T dependence of the correlation time for the spin fluctuations in $[TbPc_2]^0$ and $[DyPc_2]^0$ (in the inset, for T > T*) derived from λ data reported in Fig. (6).
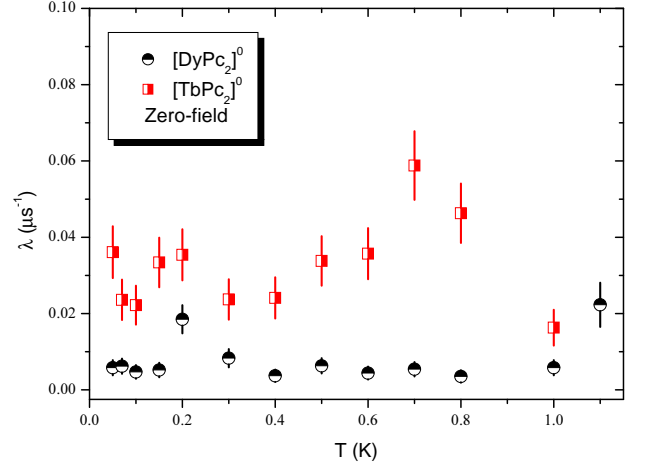

FIG. 8: T dependence of the muon relaxation rate in zero-field for $[DyPc_2]^0$ and $[TbPc_2]^0$, at T < 1 K.

by attaching 0.01 mm diameter gold wires to the samples with conductive paste and sub-μA currents were used. The samples were left free-standing to minimize thermal stress and consequent cracking. The voltage has been measured with a voltmeter with an internal impedance larger than 10 GΩ. Three different crystals have been measured and they all showed an increasing resistance on cooling from 2.5 kohm to greater than 2 Mohms below 15 K. In Fig. (9) the temperature dependence of the resistivity for a crystal with a $2.72 \cdot 10^{-3}$ area/lenght ratio is shown. The sample conducts at room temperature with a resistivity $\rho \simeq 6.4 \ \Omega \cdot cm$. Upon cooling, ρ presents an initial smooth decrease till about 220 K and then an activated growth, characterized by an activation energy $\Delta E \simeq 11 meV$, down to about 25 K.
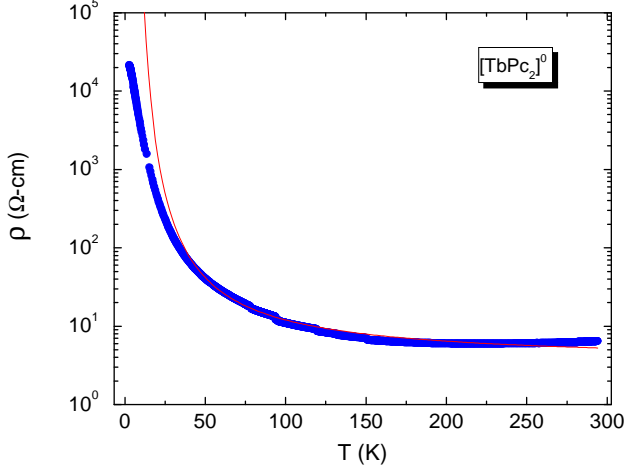
FIG. 9: Temperature dependence of resistivity ρ, measured for a $[TbPc_2]^0$ crystal. Solid line represents the best fit of the activated trend in the 220 - 30 K region.

III.   DISCUSSION AND CONCLUSIONS

First we shall discuss the temperature dependence of the static uniform susceptibility χ_S in $[DyPc_2]^0$, in order to derive the CF levels structure. Since we are dealing with a powder, the molecules and the CF axis are randomly oriented with respect to the external field $\mathbf{H} \parallel \hat{\mathbf{z}}$. Thus the total magnetization $\mathbf{M}$ can be deduced by summing the contributions of the molecules with the anisotropy axis perpendicular and parallel to $\hat{\mathbf{z}}$, namely $M(T) = \frac{2}{3}M_{x,y}(T) + \frac{1}{3}M_z(T)$, with

$$M_i(T) = N_A \frac{\sum_{k=-15/2}^{+15/2} \langle \mu_i^k \rangle e^{-\frac{E_i^k}{T}}}{\sum_{k=-15/2}^{+15/2} e^{-\frac{E_i^k}{T}}} \quad , \quad i = x, y, z \quad . \tag{1}$$

In Eq. (1), E_i^k represents the k-th eigenvalue of the hamiltonian:

$$\hat{\mathcal{H}} = \hat{\mathcal{H}}_{CF} + g\mu_B \hat{\mathbf{J}} \cdot \mathbf{H} \quad , \tag{2}$$

where $\hat{\mathcal{H}}_{CF}$ is the crystal field hamiltonian and $g\mu_B\hat{\mathbf{J}} \cdot \mathbf{H}$ is the Zeeman term. $\langle \mu_i^k \rangle$ is the expectation value of the i-th component of the magnetic moment over the k-th eigenstate of the hamiltonian. In order to analyze $\chi_S T$ we started from the CF structure for the $J = 15/2$ ground-state multiplet initially derived by Ishikawa et al. for $[DyPc_2]^- \cdot TBA^+$.[13] Then we have varied the splitting among the levels until we found the best fit of the experimental data. Two sets of possible solutions were found to fit reasonably well $\chi(T)T$ data. However, only one of them yielded a splitting between the lowest lying energy levels around 65 K, the value derived from AC susceptibility measurements (see later on). The corresponding

energy splittings are $\Delta_1 = 65$ K, corresponding to the separation between the $|m = \pm 13/2\rangle$ ground states and the $|m = \pm 9/2\rangle$ first excited levels, $\Delta_2 = 47$ K between the $|m = \pm 9/2\rangle$ levels and the $|m = \pm 11/2\rangle$ second excited levels and $\Delta_3 = 460$ K between the $|m = \pm 11/2\rangle$ levels and the $|m = \pm 15/2\rangle$ third excited levels. These values differ from the ones deduced for $[DyPc_2]^-$ on the basis of crystal field calculations ($\Delta_1 \simeq 50$ K, $\Delta_2 \simeq 207$ K, $\Delta_3 \simeq 126$ K)[13]. As it can be seen in Fig. (1), a good fit of the experimental data is found.

From the CF splittings, combined with the μSR relaxation data (Fig. (10)), it is possible to derive information on the spin-phonon coupling driving the high T spin fluctuations in $[DyPc_2]^0$. Since the energy difference between the muon hyperfine levels and the m levels of Dy^{3+} spin is large, the muon longitudinal relaxation rate λ is driven by an indirect relaxation mechanism involving a muon spin flip without change in m. This is possible thanks to the tensorial nature of the hyperfine coupling constant, which allows the coupling of the transverse components of the hyperfine field $h_{x,y}$ to J_z. Thus, denoting with (τ_m) the finite life-time of the crystal field levels induced by the spin-phonon scattering processes, λ can be written in the form[17]

$$\lambda = \frac{\gamma_\mu^2 \langle \Delta h_\perp^2 \rangle}{Z} \sum_{m=-15/2}^{+15/2} \frac{\tau_m e^{-E_m/T}}{1 + \omega_L^2 \tau_m^2} \quad , \tag{3}$$

E_m being the eigenvalues of the CF levels and Z is the corresponding partition function. It is noted that the low magnetic field (1000 Gauss) applied during μSR experiments yields a negligible correction to E_m and, hence, its effect is negible for $k_B T \gg \mu_B H$. The life-time for the m levels can be expressed in terms of the transition probabilities $p_{m,m\pm1}$ between m and $m \pm 1$ levels, which depend on the CF eigenvalues and on the spin-phonon coupling constant C[18]:

$$\frac{1}{\tau_m} = p_{m,m-1} + p_{m,m+1} \quad , \tag{4}$$

$$p_{m,m\pm1} = C \frac{(E_{m\pm1} - E_m)^3}{e^{(E_{m\pm1} - E_m)/T} - 1} \tag{5}$$

Now the temperature dependent muon relaxation rate can be correctly fit using Eqs.3-5 (Fig. 10) by considering the CF level splitting previously estimated from $\chi_S T$ fit and by using three different spin-phonon constants C_1 and $C_2 \rightarrow 0$, while $C_3 \simeq 2000$ Hz/K^3, which should be associated with the transitions $|m = \pm 11/2\rangle \leftrightarrow |m = \pm 13/2\rangle$, $|m = \pm 9/2\rangle \leftrightarrow |m = \pm 11/2\rangle$ and $|m = \pm 15/2\rangle \leftrightarrow |m = \pm 13/2\rangle$, respectively. We remark that C increases with the energy jump involved in the transition. This suggests that the relevant processes driving the transitions preferentially involve high energy vibrational modes.
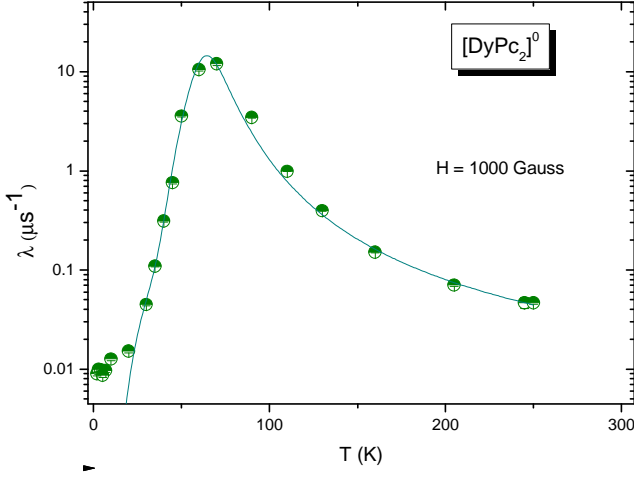
FIG. 10: Temperature dependence of the muon longitudinal relaxation rate in $[DyPc_2]^0$ for H = 1000 Gauss (circles). The line is the best fit according to Eqs. (3, 5).

In Fig.(10) one can notice that the best fit according to Eq.3 reproduces the muon relaxation data very well for T > 25 K. Since in this model only the thermally activated spin excitations are concerned, the behaviour of $\lambda(T)$ below 25 K should be probably ascribed to different processes. For instance also in $\chi_S T$ a discrepancy from the theoretical calculation is observed at very low T. In fact, for T < 4 K $\chi_S T$ abruptly upturns, possibly signaling the onset of intermolecular correlations. In order to clarify this point, μSR experiments have been performed down to very low T in $[DyPc_2]^0$ and $[TbPc_2]^0$ compounds, as shown in Fig. 6. As noted earlier, while the muon relaxation rate is nearly T-independent below 1 K for both complexes (at least down to 50 mK), the very weak maxima located at $T = 0.2$ K and 0.7 K for the Dy and Tb samples, respectively, may in fact signal an onset of these intermolecular correlations.

Now we turn to the comparison of the μSR and AC susceptibility results. The maxima in χ''/χ_S shifting to lower temperature upon decreasing the irradiation frequency clearly indicate a progressive slowing down of the dynamics on cooling. In the case of a monodispersive dynamical relaxation mode, at the peak temperature (T_m) the bulk magnetization relaxation time $\tau_c(T_m)$ matches the inverse of the angular frequency ω of the applied oscillating field, according to the expression

$$\chi''(\omega) = \frac{\chi_S \omega \tau_c}{1 + \omega^2 \tau_c^2} \quad , \qquad (6)$$

We have checked the validity of this expression by performing frequency scans at a fixed temperature and found that in the explored T range the above expression was satisfied. The linear relation of $ln(\tau_c(T_m)^{-1})$ to $1/T$ (Fig. 11) indicates that the Orbach process is dominant in the high temperature range and that the Arrhenius law $\tau_c = \tau_0 exp(\Delta/T)$ for the correlation time is obeyed. From the fit of $[TbPc_2]^0$ data in Fig.11 one estimates a value for the energy barrier $\Delta \simeq 750K$, slightly smaller than the one deduced from muon relaxation rate measurements[12] in the same sample. On the other hand it should be remarked that this value is much larger than the one reported by Ishikawa et al. ($\Delta \simeq 590$ K) in the same nominal compound.[9] The fit of $[DyPc_2]^0$ data in Fig.11 gives a much smaller activation energy $\Delta \simeq 65$ K, which corresponds quite well to the one obtained from the analysis of the static susceptibility data in Fig.(1), and provides an estimate for the separation among the lowest energy levels of $[DyPc_2]^0$. This value is much different with the barrier estimated from μSR relaxation at higher temperature, which yields an estimate for the energy separation among the high energy levels.[12]
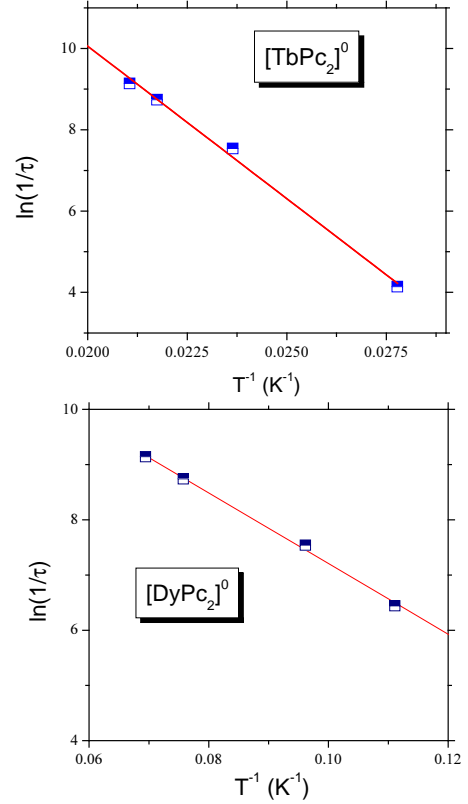

FIG. 11: Natural logarithm of the spin correlation rate against the inverse of the χ''/χ_S peak temperature for $[TbPc_2]^0$ ($H = 1000$ Gauss) (top) and for $[DyPc_2]^0$ ($H = 9000$ Gauss) (bottom). The red lines correspond to the best fits for an activated behaviour for a barrier $\Delta = 750$ K for $[TbPc_2]^0$ and $\Delta = 65$ K for $[DyPc_2]^0$.

In order to better compare the T-dependence of the correlation time derived by means of AC susceptibility and μSR in $[TbPc_2]^0$ we have derived, via Eq.6, the behaviour of τ_c estimated from AC susceptibility measurements and compared to the data reported in Fig. (7), derived with μSR. As it is shown in Fig.(12) the T-dependence of τ_c derived by the two techniques at different magnetic fields overlap rather well above 45 K. At

lower temperatures a plateau is evidenced by both techniques and associated with tunneling processes among the $|m = \pm 6\rangle$ low-energy levels. It is noticed that the plateau lies at different values depending on the magnitude of the applied field and on the technique. As it has been pointed out in Ref.12 the magnetic field leads to a Zeeman splitting of the two-fold degenerate ground-state and causes a reduction of the tunneling rate. Although this justifies the progressive increase of τ_c with magnetic field observed by each technique, it cannot explain the significant difference in the τ_c values deduced by μSR and AC susceptibility in the low-temperature tunneling regime. Thus, while both techniques probe the same high temperature activated dynamics driven by spin-phonon coupling, the low-temperature tunneling dynamics probed at the microscopic or at the macroscopic level are different. This suggests that there is some correlation among the magnetic moments in the different molecular units which cause fluctuations which do not affect the total magnetization. This coupling should lead to flip-flop like fluctuations[19] yielding a magnetic moment flip from $|m = +6\rangle$ to $|m = -6\rangle$ on one molecule and the opposite flip in the adjacent molecule. These processes, which cannot be accounted for by a direct dipolar coupling among Tb^{3+} spins since they produce a change $\Delta m = \pm 12$, do not yield a net variation in the total magnetization and, hence, do not contribute to the AC susceptibility. In other words, at low-T μSR probes T_2-like processes involving the fluctuations of Tb^{3+} moments while AC susceptibility probes only those T_1-like processes yielding a net variation of the macroscopic magnetization. The precise nature of these fluctuations, similar to the ones involving phonon trapping in Ni10,[20] still has to be clarified.
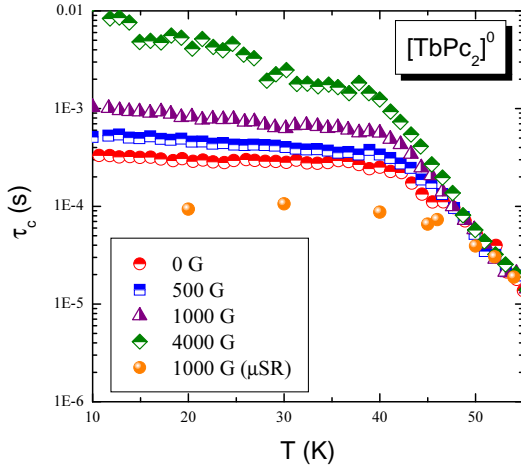

FIG. 12: Temperature dependence of τ_c, deduced from Eq.(6) for a static field of 0, 500, 1000, 4000 Gauss in $[TbPc_2]^0$ compound. Solid circles correspond to τ_c temperature dependence as derived from μSR analysis.

Finally, we turn to the discussion of transport properties. As it is shown in Fig.(9), the temperature dependence of the resistivity is characterized by a rather small energy barrier, around 11 meV. Now, in $[TbPc_2]^0$ molecular orbital calculations[21] show that there is one unpaired electron in the a_2 highest occupied molecular orbital (HOMO), basically involving orbitals from the carbon atoms at the center of the Pc rings. If there is a sufficient overlap between the a_2 orbitals of the adjacent molecules, which are stacked forming chains, electron delocalization and a metallic behaviour should be attained. However, in those Pc-based systems the electron correlations are significant, particularly at half-band filling[22], and the on-site Coulomb repulsion U can overcome the hopping integral t among adjacent molecules leading to a Hubbard insulating behaviour. Hence, the activated behaviour of the resistivity should be ascribed to correlation effects rather than to the band structure, which should typically lead to much larger activation energies. The band structure and, accordingly, the hopping integral t appear to sizeably depend on the local structure, in particular, on the buckling of the Pc ring plane and on the rotation of adjacent Pc rings, hence it is possible that at high T the crossover from a negative to a positive $d\rho/dT$ with increasing T, might be ascribed to those structural effects.

In conclusion, we have clearly shown that both AC susceptibility and μSR probe a high T activated spin dynamics in neutral $[LnPc_2]$ molecular magnets, characterized by quantitatively similar correlation times. At low temperature both techniques exhibit a flattening of the correlation time which is associated with tunneling processes. Nevertheless, from μSR one estimates correlation times which are one order of magnitude shorter than the ones derived by AC susceptibility measurements. This discrepancy between microscopic and macroscopic techniques indicates that there must be some correlation among Tb^{3+} moments, which cause fluctuations which do not contribute to the uniform macroscopic susceptibility. The analysis of the static uniform susceptibility and of the μSR relaxation rates in $[DyPc_2]^0$ have allowed for a better characterization of the CF splitting of the $J = 15/2$ multiplet and of the spin-phonon couplings driving the activated dynamics in this compound than was reported in Ref.13. Finally, we have reported the behaviour of the resistivity in $[TbPc_2]^0$, where a low T activated behaviour, possibly arising from electron-electron Hubbard-like correlations, is evidenced.

[1] L. Bogani and W. Wernsdorfer, *Nat. Mater.* **7** 179 (2008)

[2] M. Leuenberg and D. Loss, *Nature* **410** 789 (2001)

[3] A. K. Ekert and R. Jozsa, *Rev. Mod. Phys.* **68** 733 (1996)

[4] S. Klyatskaya, J.R. Galán Mascarós, L. Bogani, F. Hennrich, M. Kappes, W. Wernsdorfer and M. Ruben, J. Am. Chem. Soc. 131, 15143 (2009)

[5] L. Vitali, S. Fabris, A. Mosca Conte, S. Brink, M. Ruben, S. Baroni and K. Kern , Nano Lett. 8, 3364 (2008).

[6] B. Cage, S. E. Russek, R. Shoemaker, A. J. Barker, C. Stoldt, V. Ramachandaran and N. S. Dalal, *Polyhedron* **26** 2413 (2007)

[7] N. Ishikawa, M. Sugita, T. Ishikawa, S. Koshihara and Y. Kaizu, *J. Phys. Chem. B* **108** 11265 (2004)

[8] F. Branzoli, P. Carretta, M. Filibian, G. Zoppellaro, M. J. Graf, J. R. Galan-Mascaros, O. Fuhr, S. Brink and M. Ruben, *J. Am. Chem. Soc.* **131** 4387 (2009)

[9] N. Ishikawa, M. Sugita, N. Tanaka, T. Ishikawa, S. Koshihara and Y. Kaizu, *Inorg. Chem.* **43** 5498 (2004)

[10] S. Takamatsu, T. Ishikawa, S. Koshihara and N. Ishikawa, *Inorg. Chem.* **46** 7250 (2007)

[11] N. Ishikawa, Y. Mizuno, S. Takamatsu, T. Ishikawa and S. Koshihara, *Inorg. Chem.* **47** 10217 (2008)

[12] F. Branzoli, M. Filibian, P. Carretta, M. Ruben and S. Klyatskaya, *Phys. Rev. B* **79** 220404 (2009)

[13] N. Ishikawa, M. Sugita, T. Okubo, N. Tanaka, T. Iino and Y. Kaizu, Inorg. Chem. 42, 2440 (2003)

[14] M. Moussavi, A. De Cian, J. Fischer and R. Weiss, *Inorg. Chem.* **27**, 1287 (1988); N. Koike, H. Uekusa, Y. Ohashi, C. Harnoode, F. Kitamura, T. Ohsaka and K. Tokuda, *ibid.* **35**, 5798 (1996); K. Kasuga, M. Tsutsui, R. C. Petterson, K. Tatsumi, N. Van Opdenbosch, G. Pepe and E. F. Meyer, *J. Am. Chem. Soc.* **102**, 4835 (1980).

[15] K. Katoh, Y. Yoshida, M. Yamashita, H. Miyasaka, B.K. Breedlove, T. Kajiwara, S. Takaishi, N. Ishikawa, H. Isshiki, Y.F. Zhang, T. Komeda, M. Yamagishi and J. Takeya, J. Am. Chem. Soc. 131, 9967 (2009)

[16] A. Schenck, *Muon Spin Rotation: Principles and Applications in Solid State Physics* (Hilger, Bristol, 1986).

[17] A. Lascialfari, Z. H. Jang, F. Borsa, P. Carretta and D. Gatteschi, *Phys. Rev. Lett.* **81** 3773 (1998)

[18] J. Villain, F. Hartmann-Boutron, R. Sessoli and A. Rettori, *Europhys. Lett.* **27** 159 (1994)

[19] A. Abragam in *Principles of Nuclear Magnetism* (Clarendon Press, Oxford 1961)

[20] M. Belesi, E. Micotti, M. Mariani, F. Borsa, A. Lascialfari, S. Carretta, P. Santini, G. Amoretti, E. J. L. McInnes, I. S. Tidmarsh and J. R. Hawkett, Phys. Rev. Lett. 102, 177201 (2009)

[21] R. Rousseau, R. Aroca and M.L. Rodriguez-Méndez, J. Mol. Struc. 356, 49 (1995)

[22] M. Filibian, P. Carretta, M. C. Mozzati, P. Ghigna, G. Zoppellaro, and M. Ruben, Phys. Rev. Lett. 100, 117601 (2008)